Characterization of Constitutional Liquid Film Migration in Nickel-Base Alloy 718

V.L. ACOFF and R.G. THOMPSON

When multiphase alloys are rapidly heated, it is possible to cause melting of the interface between phases. This is called constitutional liquation if, during melting, the bulk composition is in a nonliquid region of the phase diagram but the tie-line between the liquating phases passes through a liquid region. The liquid produced during constitutional liquation can spread along grain boundaries and promote liquid film migration (LFM). This is known as constitutional liquid film migration (CLFM), which is thermodynamically similar to liquid film migration; however, mechanistically there are significant differences. Nickel-base alloy 718 has been studied to show the features of migration that are unique to CLFM. Experimentation consisted of heat-treating rods of alloy 718 to promote the trapping of niobium carbide particles on the grain boundaries. These samples were then subjected to isothermal treatments above their constitutional-liquation temperature, which produced CLFM of the grain boundaries. The movement of the liquid films away from their centers of curvature, the formation of a new solid solution behind the migrated liquid films, and the reversals of curvature of the migrated liquid films confirmed that CLFM was the phenomenon observed. The concentration of niobium behind the migrated liquid films for isothermal treatments below the solidus temperature was shown to be greater than the niobium concentration in the matrix. Above the solidus temperature, there was no increase in niobium concentration. The validity of the coherency strain hypothesis as the driving force for CLFM in alloy 718 is discussed.

I. INTRODUCTION

A. Liquid Film Migration

Researchers have shown it is possible to cause grain boundaries to migrate as a result of solute atoms diffusing along the grain boundaries. [1-4] This phenomenon has been termed diffusion-induced grain-boundary migration (DIGM). Microstructural features that distinguish DIGM from curvature-driven migration are the grain boundaries often moving away from their centers of curvature and a new solid solution forming behind the migrating boundaries. [5] Similar migration characteristics may occur when the grain boundary is replaced by a liquid film. Liquid film migration (LFM) can be qualitatively considered as a variant of the DIGM process and has been shown to exhibit some of the same microstructural features as DIGM. [6,7]

Several hypotheses have been proposed for the driving force for LFM. A hypothesis that explains many of the experimental observations by previous researchers is the coherency strain hypothesis, ^[8] According to the coherency strain hypothesis, when a solute-rich liquid comes into contact with the solid matrix, the solute atoms diffuse from the liquid into the matrix and cause a coherency strain due to the difference in size between the matrix and solute atoms. This strain causes a shift in the free-energy curve for the liquid-matrix interface on that side of the film where coherency persists or is greatest. ^[9] A transverse composition

gradient in the liquid film occurs as a result of the effect of coherency strain on the free-energy curve. Migration of the liquid film then occurs to maintain the interface compositions in the presence of flux solute down the concentration gradient in the liquid. LFM has been observed in a number of alloy systems.^[10-16]

B. Constitutional Liquid Film Migration

Radhakrishnan and Thompson^[17] were the first to report LFM occurring *in situ* in the weld heat-affected zone (HAZ) as a result of constitutional liquation. They also showed that LFM and subgrain coalescence explain most of the observed microstructural phenomena and the kinetics of grain growth in nickel alloy 718.^[18] Nakkalil *et al.*^[19] later reported LFM from constitutional liquation in the HAZ of nickel alloy 903.

Constitutional liquation can be best described in terms of a binary alloy. Consider a phase diagram like the one shown in Figure 1. If an alloy with composition C_0 is rapidly heated above its eutectic temperature T_E to a temperature T_{AD} the AB particles will not have sufficient time to dissolve. Therefore, a diffusion couple is set up between the AB particles and the matrix, which have the compositions of C_{AB} and C_{AD} respectively (Figure 1(a)). At the interface between the AB particle and the matrix, liquid forms in accordance with the phase diagram and has a composition which ranges from C_{L1} to C_{L2} (Figure 1(b)). Given sufficient time and temperature, the AB particle completely liquates and the situation in Figure 1(c) occurs. Liquid from the liquating AB particles may wet grain boundaries that it contacts, thus creating grain-boundary liquid films.

Since the AB particles would not be present under equilibrium conditions above T_E , the liquid that forms from liquating AB particles is metastable. Thus, the liquid would

Manuscript submitted January 6, 1995.

V.L. ACOFF, Assistant Professor, is with the Department of Metallurgical and Materials Engineering, University of Alabama, Tuscaloosa, AL 35487-0202. R.G. THOMPSON, Professor, is with the Department of Materials and Mechanical Engineering, University of Alabama at Birmingham, Birmingham, AL 35294-4461.

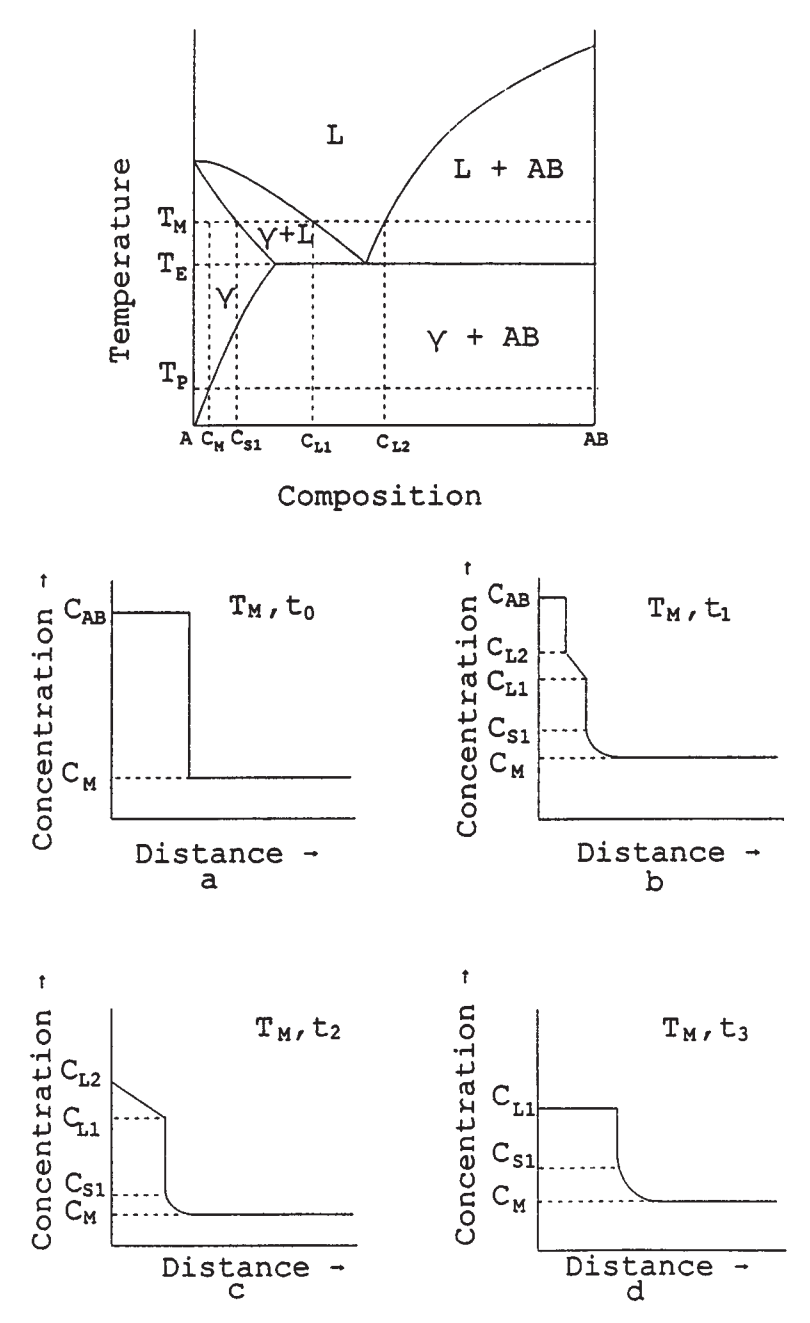


Fig. 1—Schematic of constitutional liquation of particle AB in the binary shown. (a) Initial configuration of the matrix-AB diffusion couple. (b) Concentration gradients in front of the liquating AB particle in accordance with the phase diagram. (c) The formation of metastable concentration gradient in the liquid at the end of AB liquation. (d) Elimination of the metastable concentration gradient by diffusion. (21)

eventually disappear due to back diffusion of solute into the matrix. [20] The back diffusion of solute atoms from the liquid to the matrix could cause coherency strain to develop if there is sufficient size difference between the solute and matrix atoms. This could promote the migration of liquid films. [17] Figures 1(b) and (c) depict a concentration gradient in the liquid film from the particle-liquid interface to the liquid-matrix interface. This concentration gradient may promote LFM in the same way that DIGM does, without the need for coherency strain in the matrix. However, since

the concentration gradient in the liquid is metastable, it will eventually disappear and the situation in Figure 1(d) will occur. At this point, constitutional liquid film migration (CLFM) may continue only through a coherency strain mechanism.

The phenomenon described previously, which causes liquid films to migrate as a result of the formation of a metastable liquid film, has been termed CLFM. Thermodynamically similar to LFM, CLFM is significantly different mechanistically. Features that are unique to CLFM are as follows.

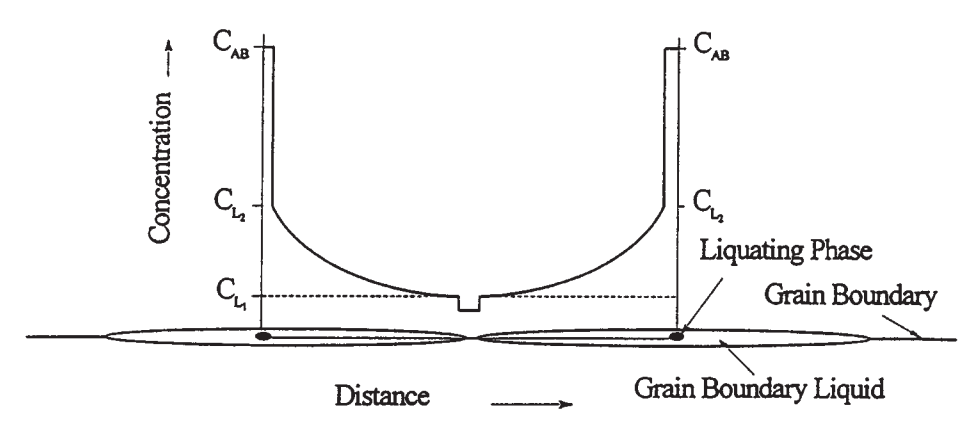


Fig. 2—Schematic of the formation of a lateral concentration gradient in the grain boundary liquid film due to the constitutional liquation of AB particles.[21]

Table I. Composition of Alloy 718 in Weight Percent

Element	Ni	Cr	Fe	Nb + Ta	Mo	Ti	Al	Co	Si	Mn	С	S	P	Cu	В
Wt pct	52.44	18.23	19.06	5.05	3.01	1.00	0.55	0.26	0.12	0.11	0.055	0.003	0.008	0.05	0.0037

- (a) The metastable liquid film results from the spreading of liquid that forms from the constitutional liquation of precipitates located on the grain boundaries.
- (b) A lateral (in-plane) diffusion flux of solutes occurs along the liquid film. This is due to the lateral concentration gradient which arises when the liquid, formed from individual particles, coalesces to form the liquid film. The result is a lateral concentration gradient in the liquid films that ranges from C_{L1} to C_{L2} as shown in Figures 1(b) and (c) and 2.^[21] This lateral concentration gradient is in addition to the curvature-dependent lateral concentration gradient described by Brechet and Purdy.^[22]

As observed by the present authors^[17,23] and others,^[19] CLFM originates from discrete precipitates, which produce both an in-plane solute flux as found in DIGM and a soluterich liquid as found in LFM. Therefore, the driving force for CLFM could come from either or both a lateral (in-plane) or transverse (coherent strain) solute flux.

C. Objective

Since LFM was observed to occur *in situ* in the weld HAZ of multiphase alloys due to constitutional liquation, it is important that this phenomenon be better understood. To date, there has been no systematic investigation of CLFM. It is the purpose of this study to investigate LFM accompanying constitutional liquation in alloy 718 in order to gain a better understanding of the conditions under which this phenomenon occurs. The objective of this study was to determine if the migrating interface could be characterized by equilibrium-phase diagram predictions.

II. EXPERIMENTAL PROCEDURE

A. Material

Alloy 718 is a nickel-base superalloy that mainly consists of a face-centered-cubic (fcc) solid solution of nickel, iron, and chromium with a significant amount of molybdenum and niobium. The alloy 718 used in this study was received

in the solution-treated condition. The material was in the form of a hot-rolled rod, 1.295 cm (0.510 in.) in diameter that was cut into samples approximately 10.16 cm (4 in.) in length. The composition of the alloy is shown in Table I. This material was chosen for study because it was known to produce significant CLFM, and importantly, it was available in a size and quantity for use in our experimental test apparatus.

B. Heat Treatment

The samples were placed inside stainless steel bags and solution treated at 1093 °C for 30 minutes followed by water quenching. The samples were then held at 650 °C for 4 hours followed by air cooling. The 650 °C heat treatment was used to promote the trapping of niobium carbide particles on the grain boundaries.

C. CLFM Thermal Treatments

A type K thermocouple was percussion welded to the midsection of the samples. In order to promote CLFM, the samples were subjected to rapid thermal cycles (recorded by the thermocouples) using a Gleeble 1000 thermomechanical device. Samples were heated at 100 °C per second to a peak temperature of 1227 °C and held isothermally for 4 seconds followed by water quenching. This procedure was repeated for different samples using peak temperatures of 1240 °C, 1250 °C, and 1260 °C. After the CLFM thermal treatments, the samples were sectioned at the location of the control thermocouple and one part was used for analysis on a JEOL* JEM-2000FX transmission electron micro-

scope (TEM) and the other was used for analysis on a light microscope and a PHILIPS** 515 scanning electron micro-

scope (SEM).

670

^{*}JEOL is a trademark of Japan Electron Optics Ltd., Tokyo.

^{**}PHILIPS is a trademark of Philips Electronic Instruments Corp., Mahwah, NJ.

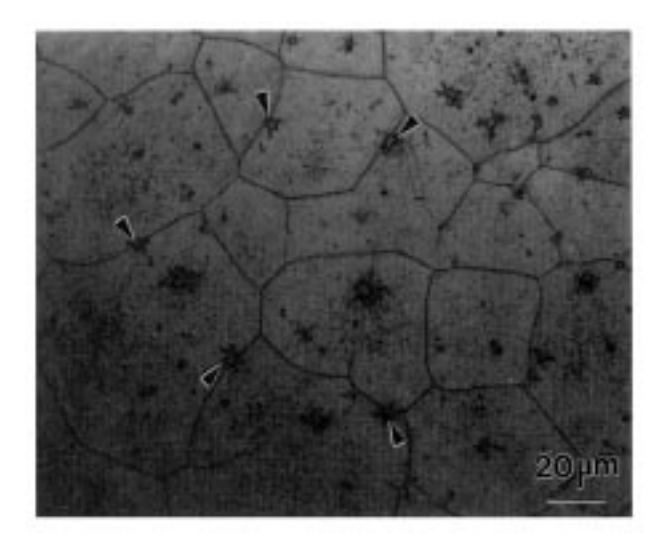


Fig. 3—Light microscope image showing the microstructure of alloy 718 after the 650 $^{\circ}$ C for 4 h heat treatment. The arrows point to niobium carbides on the grain boundaries.

D. Electron Backscatter Pattern System Analysis

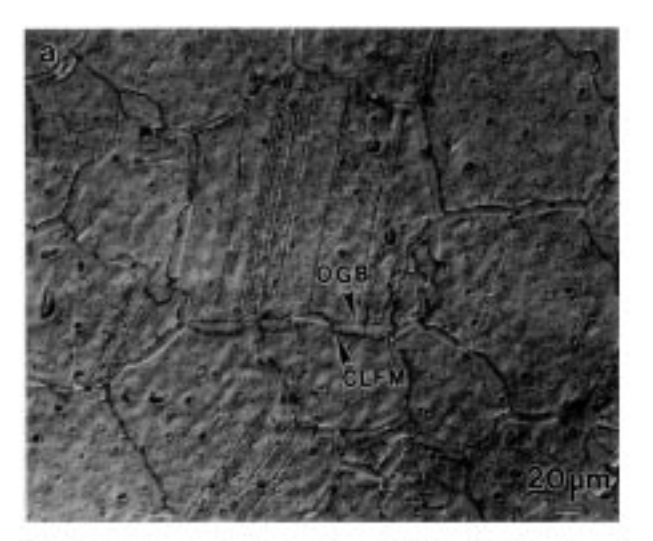
Samples were prepared for light microscopy and for evaluation on an SEM equipped with an electron backscatter pattern (EBSP) system by using conventional metallographic procedures. Etching was performed electrolytically using 10 pct oxalic acid. The conditions were 6 V and 25 seconds. Kikuchi electron backscattered diffraction patterns were obtained only from grain pairs that were separated by liquid films that exhibited reversals of curvature. A pattern was obtained from each grain in the pair. The data from these patterns were then entered into the EBSP system software, which determined the rotation angle and rotation axis between the two grains. This procedure was repeated for 90 pairs of grains that were separated by liquid films exhibiting reversals of curvature.

E. Transmission Electron Microscopy

Samples were evaluated on a JEOL JEM-2000FX TEM operated at 200 kV and equipped with an energy-dispersive X-ray spectrometer (EDS) system. The thinning electrolyte consisted of 90 pct acetic acid and 10 pct perchloric acid with thinning conditions of 50 volts and 8 °C. The TEM/EDS profiles were obtained for each temperature. From the TEM analysis, the niobium concentration in the migrated regions relative to that in the matrix was determined. There were no standards used in the TEM/EDS analysis for determining the semiquantitative values of the niobium concentration.

F. Scanning Auger Microprobe

A scanning Auger microprobe (SAM) was also used in order to detect any changes in concentration of light elements such as carbon, boron, and nitrogen that are not detectable using TEM/EDS analysis. Samples exhibiting CLFM were loaded into the SAM. The surface of the sample was cleaned by sputtering with argon ions. Following sputtering, the surfaces were immediately analyzed.



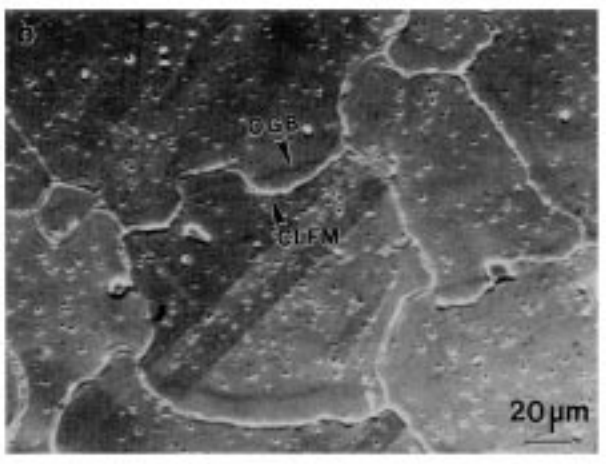


Fig. 4—(a) Light micrograph and (b) SEM micrograph of 1227 °C peak temperature sample showing the original grain boundary (OGB) position and a liquid film with reversed curvature as a result of CLFM.

III. RESULTS AND DISCUSSION

A. As-Heat-Treated Microstructure

The as-heat-treated microstructure consisted of large grains (γ matrix) with intergranular and intragranular niobium carbide particles. Heat treatment at 650 °C for 4 hours promoted trapping of some niobium carbide particles on the grain boundaries. Figure 3 shows the microstructure of alloy 718 after the 650 °C for 4 hours of heat treatment. The arrows point to niobium carbide particles on the grain boundaries.

B. Confirmation of Constitutional Liquid Film Migration

1. Movement away from center of curvature

The rapid thermal cycles produced in the Gleeble 1000 did promote CLFM in the alloy of this study for peak temperatures of 1227 °C (Figure 4), 1240 °C (Figure 5), and 1250 °C (Figure 6). The original grain-boundary position is denoted by OGB and the migrated liquid film is denoted as CLFM in Figures 4 through 6. The original grain-boundary position was defined as the area that separated the clear, clean region from the particle-containing region, which has a mottled appearance. The clear regions are the areas that



Fig. 5—Light micrograph of 1240 °C peak temperature sample showing the OGB position and a liquid film with reversed curvature as a result of CLFM.



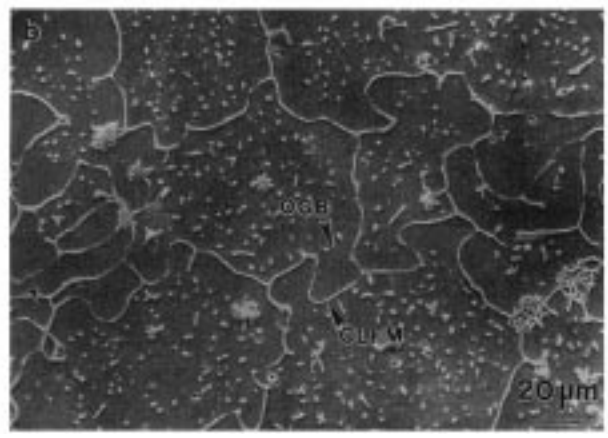


Fig. 6—(a) Light micrograph and (b) SEM micrograph of 1250 °C peak temperature sample showing the OGB position and a liquid film with reversed curvature as a result of CLFM.

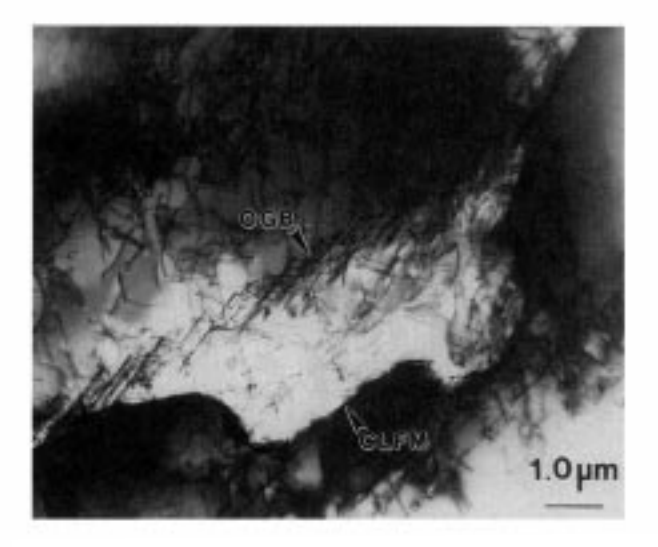


Fig. 7—TEM bright-field image of 1227 °C peak temperature sample showing area where TEM/EDS profiles where obtained.

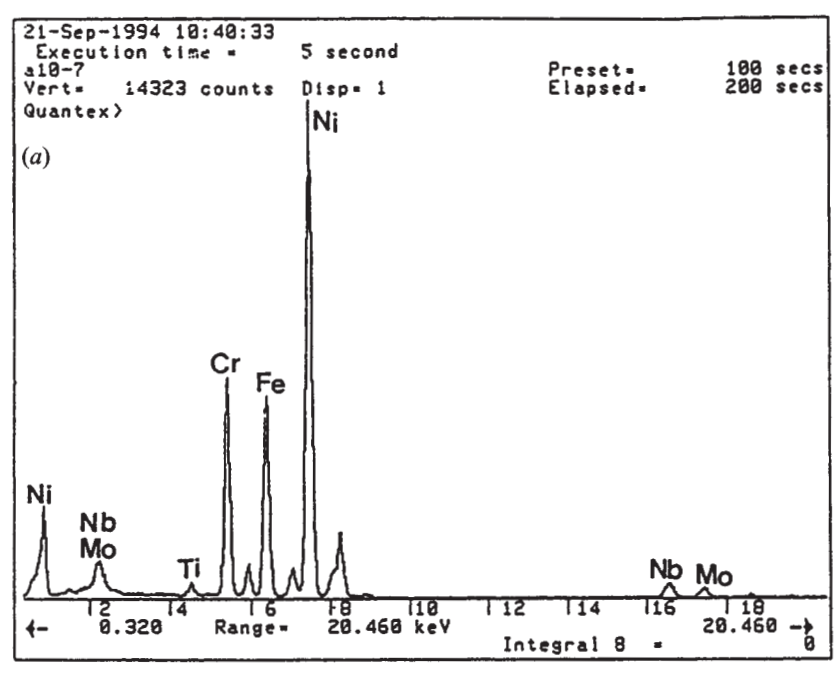
were swept by the migrated liquid film. The CLFM was confirmed by the fact that the liquid films moved away from their centers of curvature. The migration away from curvature means that there must be a driving force which overcomes the curvature-driven migration normally observed.

2. Formation of a new solid solution

Another feature that confirmed CLFM was the formation of a new solid solution behind the migrated liquid film. The formation of a new solid solution was evident from the observation that the migrated regions (areas swept by moving liquid films) etched differently from the matrix. Figure 6(b) is a representative SEM micrograph for the 1250 °C sample. This micrograph clearly shows the migrated regions are different in appearance from the matrix. This contrast, which occurs between the migrated region and the matrix, has been attributed to a variation in etch contrast due to the composition change in the newly formed solid region located near the migrated liquid film. [67,10,11,17,19] The study of EDS spectra from TEM samples also confirmed that the regions swept by migrating liquid films produced solute enrichment.

The TEM bright-field image of CLFM in the sample heated to 1227 °C for 4 seconds is shown in Figure 7. This micrograph shows the areas where TEM/EDS profiles were obtained. Representative TEM/EDS spectra from the matrix and the migrated region (area behind the migrated liquid film) are shown in Figure 8. These spectra show that the concentration of niobium in the migrated region was higher than the niobium concentration in the matrix. A plot of the niobium concentration as a function of distance is shown in Figure 9. The average niobium concentration in weight percent was 9.3 pct (range 7.6 to 10.6) for the migrated region and 5.9 pct (range 5.7 to 6.4) for the matrix.

The TEM bright-field image of CLFM in the sample heated to 1240 °C for 4 seconds is shown in Figure 10(a). The line profiles where TEM/EDS analysis was performed are shown in the TEM bright-field image. The TEM/EDS spectra from the matrix and migrated region were similar to those determined for 1227 °C. The plots for niobium



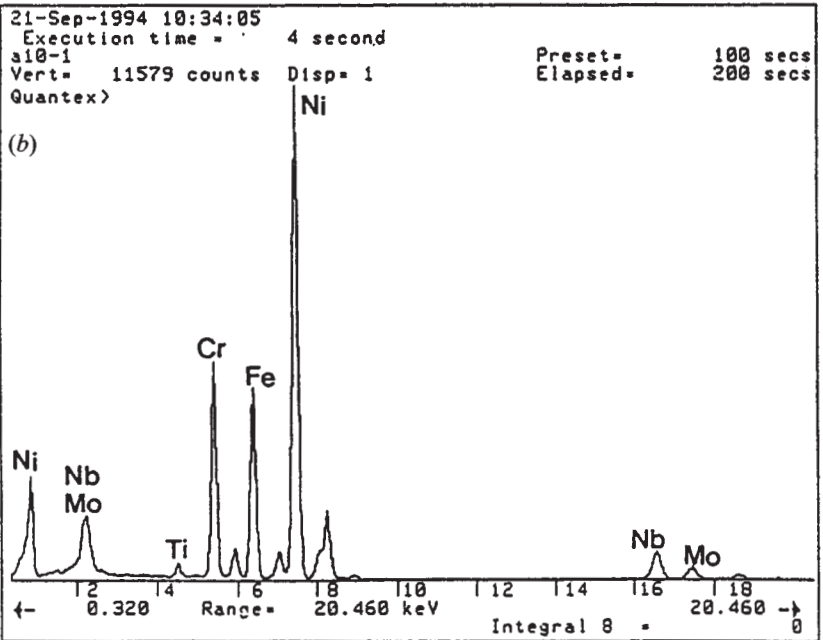


Fig. 8—Representative TEM/EDS spectra from the (a) matrix and (b) migrated region of the 1227 °C peak temperature sample.

concentration as a function of distance are shown in Figures 11 through 13, which were collected along points on data lines 1 through 3, respectively, in Figure 10(a). Since the original grain boundary positions cannot be seen in the TEM image, an SEM secondary electron image (Figure 10(b)) is shown that has a region similar to the area depicted in the TEM image. The micrographs were taken at very different magnifications and thus a direct comparison of the two is not attempted. However, the SEM micrograph is only used for illustrative purposes to suggest where the

original grain-boundary positions exist in the TEM image. Data lines are drawn in Figure 10(b), which clearly show how the TEM/EDS line profiles could have gone through more than one migrated region, as described in the following paragraph using the TEM micrograph in Figure 10(a).

Observe data line 1 drawn in Figure 10(a). This data line goes through a migrated region that is located to the left of the migrated liquid film. The concentration of niobium in this region is denoted on the plot in Figure 11 by points 0 through 5 on the x-axis. At point 6 on the x-axis, the data

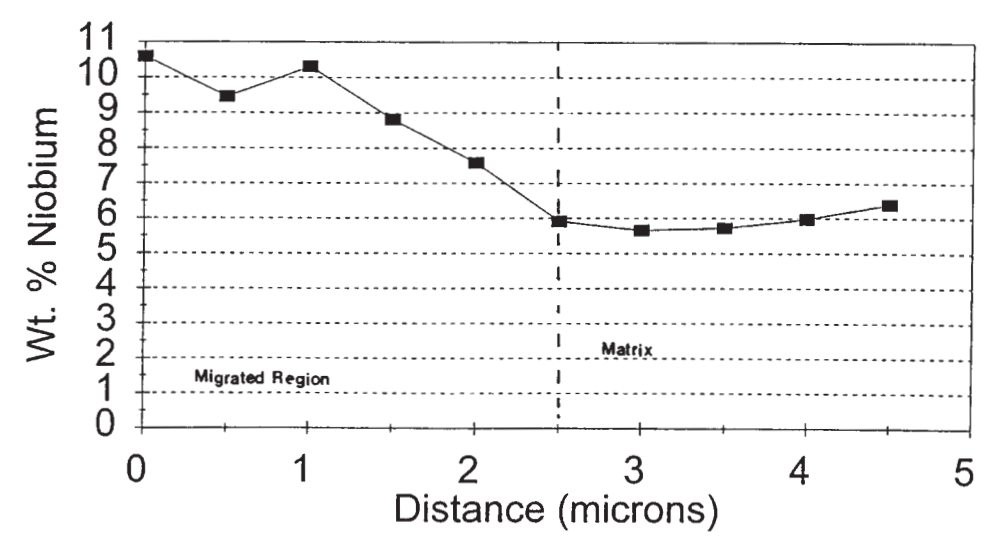
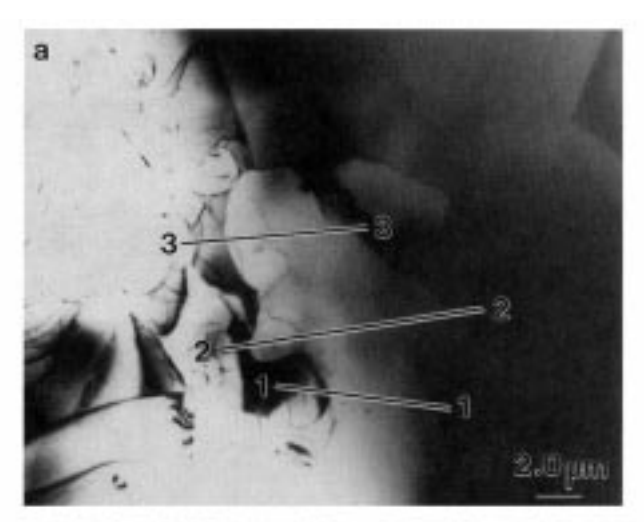


Fig. 9—Niobium concentration vs distance profile for the 1227 °C sample.



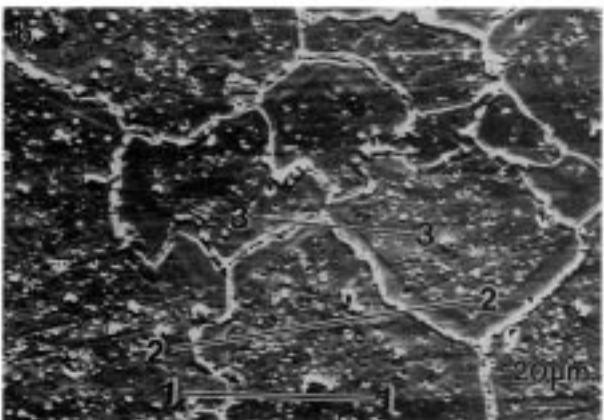


Fig. 10—(a) TEM bright-field image showing area where TEM/EDS profiles were obtained for the 1240 °C peak temperature sample. (b) SEM secondary electron image of a region similar to that shown in (a).

line goes through the matrix located to the right of the migrated liquid film. The niobium concentration vs distance

plot for data line 2 (Figure 12) shown in Figure 10(a) suggests the EDS profile obtained along data line 2 went through a migrated region, the matrix, then through another migrated region. This was postulated since the niobium concentration was relatively high from points 0 through 5 and then again between points 11 and 13, but decreased between points 6 and 10. The highest niobium concentrations are expected to occur in the migrated regions located between the original grain-boundary position and the migrated liquid film. The niobium concentration vs distance plot obtained along data line 3 in Figure 10(a) is shown in Figure 13. Figure 13 shows data line 3 went through the matrix and then through two migrated regions located adjacent to each other. Overall, the average niobium concentration for CLFM at 1240 °C for 4 seconds was determined to be 7.8 pct (range 6.0 to 9.6) in the migrated regions and 5.0 pct (range 4.1 to 5.6) in the matrix.

The niobium concentration across the migrated region and the matrix for the 1250 °C sample is shown in Figure 14 as a plot of niobium concentration vs distance. Examination of this plot shows that the niobium concentration appears to decrease slightly upon approaching the migrated liquid film. Once across the migrated liquid film, the niobium concentration drops, then increases to an approximately uniform value in the matrix. The average niobium concentration was determined to be 4.2 pct (range 3.5 to 5.0) in the migrated region and 4.0 pct (range 3.6 to 4.6) in the matrix. It is interesting to note that although the niobium concentrations in the migrated region and the matrix were relatively close, there was still an etching contrast between the two regions. This suggests that the etch contrast is not due solely to composition. Perhaps it is also due to a general alloy refinement with respect to local composition and microstructure.

3. Reversal of curvature

The CLFM was also confirmed by the reversals of curvature of the migrated liquid films that are shown in Figures 4 through 6. This reversal of curvature of the liquid films is a characteristic of LFM and has been shown to be due both to uniform and nonuniform stress relaxation mecha-

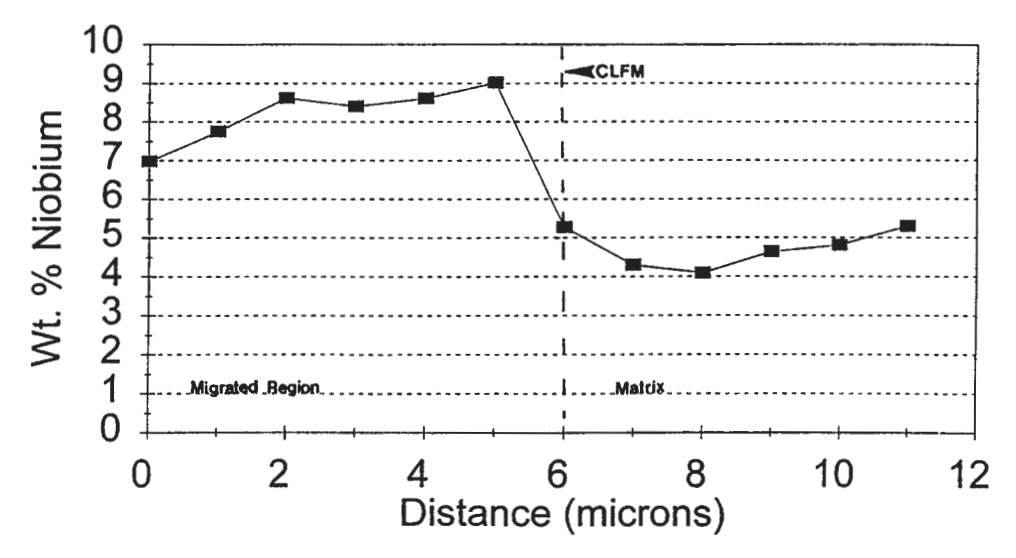


Fig. 11-Niobium concentration vs distance profile for 1240 °C collected along data line 1 shown in Fig. 10(a).

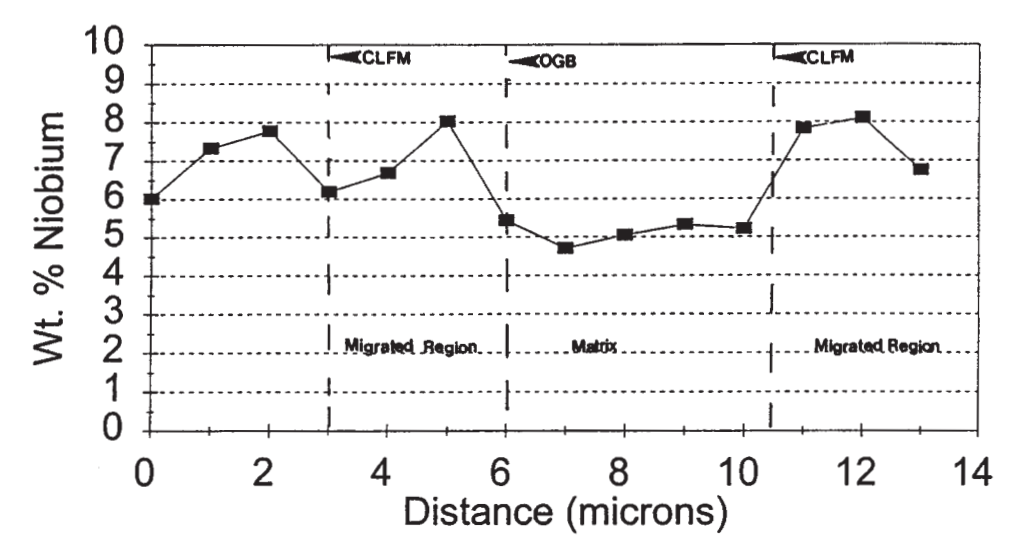


Fig. 12—Niobium concentration vs distance profile for 1240 °C collected along data line 2 shown in Fig. 10(a).

nisms.^[9] When the coherency strain becomes larger than the energy required to create dislocations in the matrix, stress relaxation occurs uniformly by plastic deformation in the matrix. This leads to a loss of coherency in the grain.^[9] Whenever a loss of coherency occurs, the migration direction reverses since there is no longer a driving force for migration in the same direction.

A loss of coherency can also occur due to a nonuniform stress relaxation across the grain boundary. The stresses due to coherency strain can relax nonuniformly by the interaction of the stress field with the existing dislocations in the matrix. If nonuniform stress relaxation occurs, migration would begin at each site of stress relaxation. This leads to the local bowing of the grain boundary at these sites of stress relaxation. That is, in this case, migration will begin at sites along the liquid film where there is local stress relaxation. Areas along the liquid film that do not have local stress relaxation will not migrate. If a liquid film has two sites of local stress relaxation that are separated by a site

that does not have local stress relaxation, the liquid film should begin to migrate at these two sites. Thus, these segments of the liquid film can migrate in opposite directions across the original grain boundary position resulting in a zigzag or "S" shaped appearance of the liquid film. This was observed in the present study for 1227 °C (Figure 4), 1240 °C (Figure 5), and 1250 °C (Figure 6).

In the TEM image for the 1227 °C sample (Figure 7), it was observed that a wall of dislocations was left at the original position of the grain boundary. Handwerker⁽⁹⁾ stated that this wall of dislocations at the original grain-boundary position occurs when the change in lattice parameter with composition is large. A wall of dislocations at the original grain boundary position was also observed by other researchers.^(3),24)

4. Influence of crystal orientation on CLFM

A total of 90 pairs of grains separated by migrated liquid films after CLFM were randomly chosen from the 1227 °C

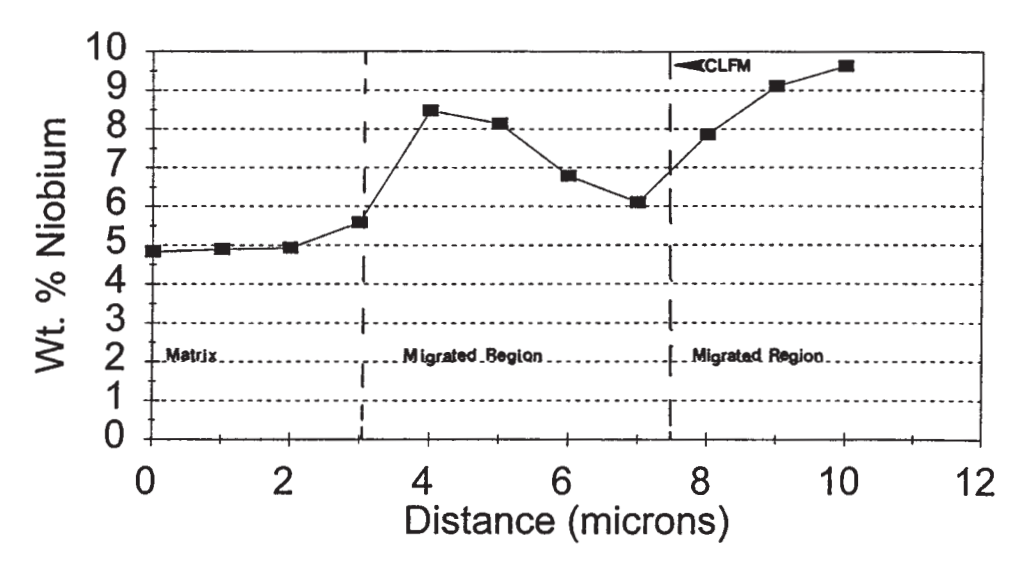


Fig. 13-Niobium concentration vs distance profile for 1240 °C collected along data line 3 shown in Fig. 10(a).

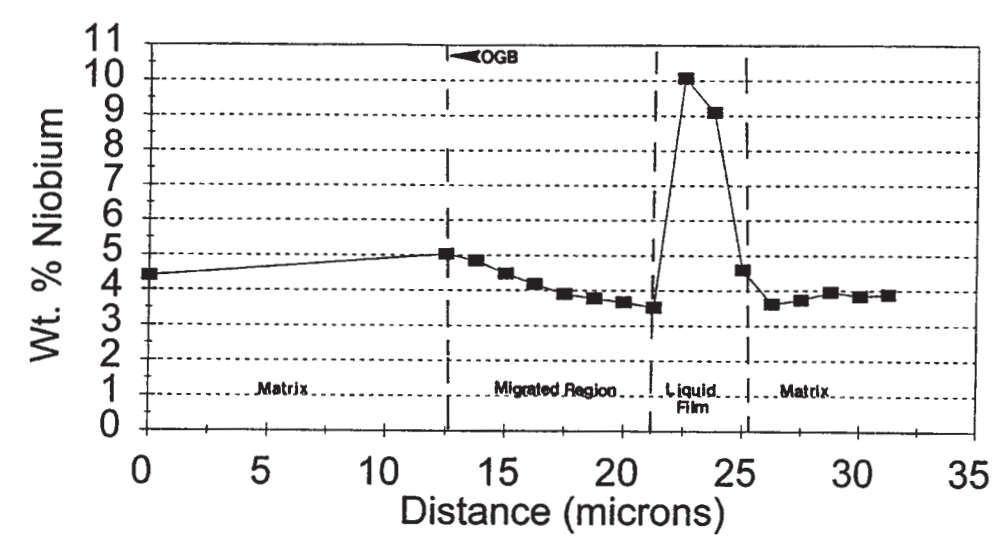


Fig. 14-Niobium concentration vs distance profile for 1250 °C.

isothermal treatment samples for EBSP analysis. All of the grains that were evaluated on the EBSP system for the crystal-orientation determination were separated by liquid films with reversed curvatures. The crystal orientations determined from EBSP analysis are given in Table II and were characterized as follows: low-angle boundaries (<15 deg), close to low-angle boundaries (15 to 20 deg), high-angle boundaries (>20 deg), and coincident site lattice (CSL) ($vv_m < 1$). All of the 90 pairs of grains were separated by migrated liquid films as a result of CLFM, showing that CLFM can occur over a large range of orientations. It can also be seen from this result that NbC precipitates can liquate and cause wetting along grains of different orientations. [23]

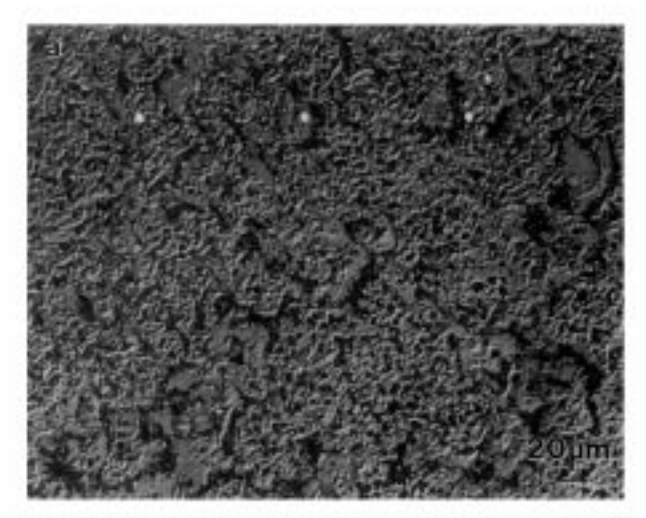
The migrated liquid films were examined in order to determine if the orientation of the grain had an effect on the direction in which the liquid film migrated. From the observation of migration on both sides of the original grain-boundary position, the crystal orientation does not restrict

Table II. Characterization of Migrated Grain Boundaries

Low Angle (<15 Deg)	Close to Low Angle (15 to 20 Deg)	High Angle (>20 Deg)	$CSL (v/v_m < 1)^*$
1	3	84	2

^{*}The term v is the angular deviation from exact CSL, and v_m is the maximum allowable deviation from exact CSL.^[25]

the migration direction.^[23] Previous researchers showed that the coherency strain was directly proportional to the orientation-dependent modulus for a given solute.^[26] Since the results of the present study show that the crystal orientation did not restrict the migration direction, the coherency strain hypothesis can not be used exclusively to explain the driving force for CLFM without mechanisms such as nonuniform stress relaxation described previously. Furthermore, the in-plane flux theory must also be considered as a possible driving force for the CLFM observed in this study.



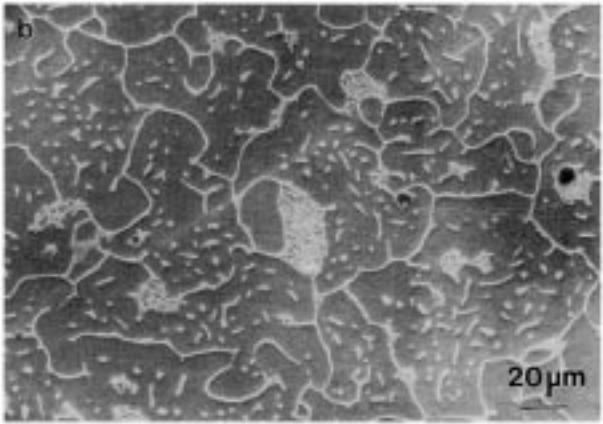


Fig. 15—(a) Light micrograph and (b) SEM secondary electron image of alloy 718 for the 1260 °C peak temperature sample.

5. Difficulty in confirming CLFM

The original grain-boundary position is indistinguishable from the matrix in the 1260 °C sample (Figure 15). The features that are characteristic of CLFM (movement away from the center of curvature, formation of a new solid solution, and reversals of curvature) were not observed. Therefore, it was difficult to confirm whether CLFM occurred at this temperature. If CLFM occurs at all at 1260 °C, it happens so quickly that it is difficult to observe before migration ceases and the system equilibrates.

C. Solute Enrichment vs CLFM Temperature

A migrating liquid film should cause alloying of the matrix at the trailing solid-liquid interface. The composition of this alloying should be given by the intersection of the phase diagram tie-line at the CLFM temperature T_M with the solidus line C_{s1} as in Figure 1. This will be true if the migrating interfaces behave in an equilibrium manner. This study made an attempt to determine this behavior for commercial alloy 718 by measuring the composition of the area swept out by the migrating liquid film as a function of temperature. If the interfaces do indeed behave in an equilibrium manner, then the composition vs temperature path for the migrated region will follow the solidus curve of the

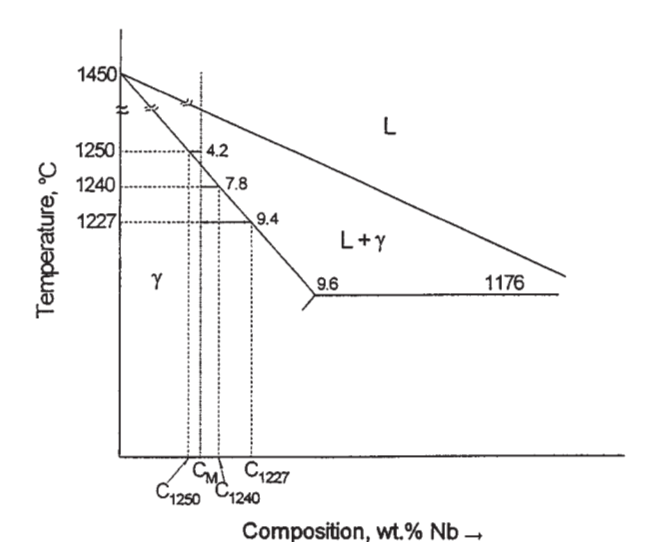


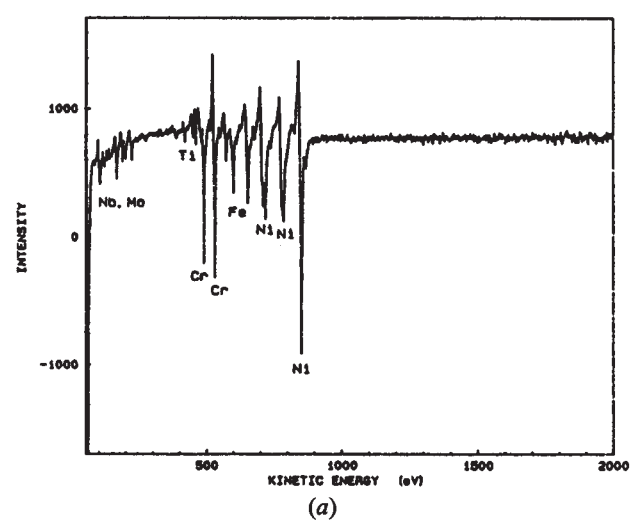
Fig. 16—Approximate γ -NbC pseudobinary phase diagram. Different peak temperatures produce different solid-liquid interface compositions during constitutional liquation. The solid composition is determined by the solidus curve, and the solute depletion or enrichment relation in the migrated zone depends on the relative position of the solidus to the matrix composition C_{Lc} .

phase diagram. Measurements showed niobium was the element that became concentrated in these migrated areas. Thus it was niobium that was followed to determine its concentration as a function of CLFM temperature.

A CLFM temperature below the alloy solidus temperature but above the eutectic temperature should result in solute enrichment. Since 1227 °C falls within this range, the niobium concentration was expected to be higher in the migrated region than in the matrix and this was found to be the case. The higher niobium concentration in the migrated region can be explained using the approximate γ -NbC pseudobinary phase diagram shown in Figure 16. This pseudobinary phase diagram was constructed from data that was obtained from work on alloy 718 by previous authors[20,27,28] and is an approximate representation of the phase relationships in nickel-base alloy 718. The melting point of γ was taken from Radhakrishnan and Thompson^[20] since the composition of the alloy 718 used in the present study was similar to the alloy 718 composition that was used in their study. However, the melting point of γ ranged from 1360 °C to 1450 °C according to the previous studies.[20,27,28] The liquidus temperature of the nominal composition was shown to range from 1260 °C to 1364 °C and the solidus temperature ranged from 1227 °C to 1320

Using this pseudobinary diagram, the 1227 °C tie-line yields a migrated zone composition designated C_{1227} . As shown on the pseudobinary diagram, C_{1227} is greater than the matrix composition denoted by C_M . Thus, niobium enrichment is predicted by the phase diagram and enrichment is found in the migrated zone of the microstructure.

As shown in Figure 4, the appearance of the microstructure for CLFM at 1227 °C confirmed that this temperature was below the solidus temperature. This was evident since no melting in the matrix was observed at this temperature. The measured semiquantitative value of niobium concen-



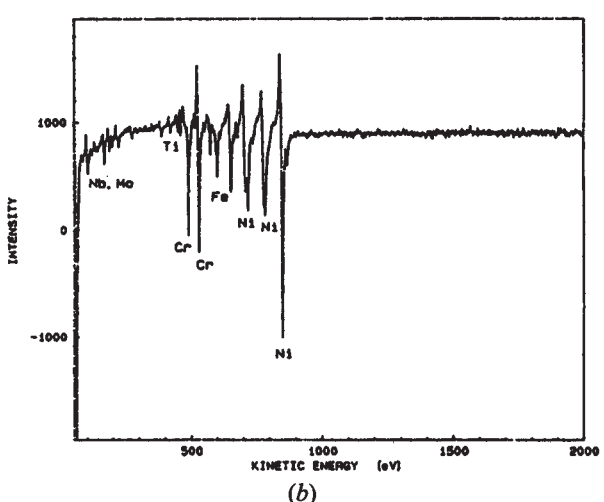


Fig. 17—Auger spectra from the (a) matrix and (b) migrated region of 1227 °C sample.

tration in the migrated region was determined to be approximately 9.4 wt pct. This falls within the range of maximum solid solubility for niobium in the matrix (7 to 10 wt pct) that was obtained from the literature. [20,27,28]

The CLFM temperature of 1240 °C should also lie between the alloy solidus temperature and the eutectic temperature. Niobium enrichment was expected and can be explained using the γ -NbC pseudobinary phase diagram in Figure 16 in the same manner as done for CLFM at 1227 °C. As shown on the pseudobinary phase diagram, C_{1240} should fall between C_M and C_{1227} . This is in agreement with the results of the present study.

The microstructure for CLFM at 1240 °C (Figure 5) showed no melting of the matrix was observed at this temperature. This suggested that 1240 °C was also below the solidus temperature for this alloy. Therefore, niobium enrichment was found to occur in accordance with the pseudobinary phase diagram for γ-NbC.

The CLFM at 1250 °C did not show niobium enrichment in the migrated region. There was no significant difference

between the niobium concentration in the migrated region and the niobium segregation in the matrix. However, observation of the niobium concentration vs distance plot for this temperature (Figure 14) showed the niobium concentration appeared to decrease slightly upon approaching the migrated liquid film. It was expected that the migrated region would be depleted of niobium since 1250 °C is believed to be above the solidus temperature for this alloy. The pseudobinary phase diagram in Figure 16 shows that the tie-line for 1250 °C yields a niobium concentration which is less than or approximately equal to the matrix composition C_M . This is in agreement with the results of the present study. The average concentration of niobium in the migrated region for CLFM at 1250 °C was 4.2 pct, which was less than the niobium concentrations that were determined for CLFM at either 1227 °C or 1240 °C.

SAM was performed on the 1227 °C and 1240 °C samples to see if segregation or depletion of carbon, boron, or nitrogen occurred in the migrated regions of these samples where niobium segregation was observed. This procedure was necessary because carbon and boron could not be detected using TEM/EDS analysis. Representative Auger spectra for the matrix and a migrated region from the 1227 °C sample are shown in Figures 17(a) and (b), respectively. The Auger spectra for the 1240 °C sample was similar to those shown for 1227 °C. Auger analysis showed no carbon, boron, or nitrogen segregation in the migrated regions. There was also no depletion of these elements in this region.

IV. CONCLUSIONS

At 1227 °C, 1240 °C, and 1250 °C, CLFM was confirmed by the following observations: the liquid films moved away from their centers of curvature, an enriched solid solution was formed in the area swept out by the migrated liquid films at 1227 °C and 1240 °C; and the migrated liquid films exhibited reversals of curvature.

The niobium concentration in the areas swept out by the CLFM decreased as a function of increasing temperature. This proved to be in accordance with the solidus curve for the γ -NbC pseudobinary phase diagram. The good correspondence between the niobium concentration and the solidus curve suggests that the migrating films behave in a manner consistent with equilibrium-phase diagram constructions.

Finally, CLFM can occur in a large number of crystal orientations as evidenced by the migration seen on both sides of the grain pairs. This suggests that both lateral and transverse solute fluxes may be important contributors to the force driving CLFM.

ACKNOWLEDGMENTS

The authors wish to thank the Department of Energy for support under Grant No. DE-FG05-91ER45449. They also greatly appreciate the hard work of Jinhua Gao, Aaron Zhou, and Brett Boutwell in producing text and figures. Discussions with Dr. B. Radhakrishnan helped to clarify many points in the analysis. The views expressed in this

article are not necessarily those of the Department of Energy.

REFERENCES

- 1. M.S. Sulonen: Acta Metall., 1960, vol. 8, pp. 669-76.
- 2. F.J.A. Den Broeder: Acta Metall., 1972, vol. 20, pp. 319-32.
- 3. M. Hillert and G.R. Purdy: Acta Metall., 1978, vol. 26, pp. 333-40.
- R.W. Balluffi and J.W. Cahn: Acta Metall., 1981, vol. 29, pp. 493-500.
- 5. D.N. Yoon: Ann. Rev. Mater. Sci., 1989, vol. 19, pp. 43-58.
- D.N. Yoon and W.J. Huppmann: Acta Metall., 1979, vol. 27, pp. 973-77.
- Y. Song, S. Ahn, and D.N. Yoon: Acta Metall., 1985, vol. 33, pp. 1907-10.
- 8. M. Hillert: Scripta Metall., 1983, vol. 17, pp. 237-40.
- C.A. Handwerker: in Diffusion Phenomena in Thin Films and Microelectronic Materials, D. Gupta and P.S. Ho, eds., Noyes Publications, Park Ridge, NJ, 1987, pp. 245-322.
- 10. Y.J. Baik and D.N. Yoon: Acta Metall., 1985, vol. 33, pp. 1911-17.
- 11. Y.J. Baik and D.N. Yoon: Acta Metall., 1986, vol. 34, pp. 2039-44.
- W.H. Rhee, Y. Song, and D.N. Yoon: Acta Metall., 1987, vol. 35, pp. 57-60.
- 13. W.H. Rhee and D.N. Yoon: Acta Metall., 1987, vol. 35, pp. 1447-51.
- 14. W.H. Rhee and D.N. Yoon: Acta Metall., 1989, vol. 37, pp. 221-28.

- 15. Y.J. Baik and D.N. Yoon: Acta Metall., 1990, vol. 38, pp. 1525-34.
- M. Kuo and R.A. Fournelle: Acta Metall., 1991, vol. 39, pp. 2835-45
- B. Radhakrishnan and R.G. Thompson: Scripta Metall., 1990, vol. 24, pp. 537-42.
- B. Radhakrishnan and R.G. Thompson: Metall. Trans. A, 1993, vol. 24A, pp. 2773-85.
- R. Nakkalil, N.L. Richards, and M.C. Chaturvedi: Scripta Metall., 1992, vol. 26, pp. 1599-1604.
- B. Radhakrishnan and R.G. Thompson: Metall. Trans. A, 1992, vol. 23A, pp. 1783-99.
- B. Radhakrishnan: Ph.D. Dissertation, The University of Alabama at Birmingham, Birmingham, AL, 1989.
- 22. Y. Brechet and G.R. Purdy: Scripta Metall., 1988, vol. 22, pp. 1629-
- V.L. Acoff, R.G. Thompson, and R.D. Griffin: in Proc. Solid—Solid Phase Transformations Conf., TMS, Warrendale, PA, 1994, pp. 1207-12
- Z. Guan, G. Liu, and J. Du: Acta Metall., 1993, vol. 41, pp. 1293-1300.
- V. Randle: The Measurement of Grain Boundary Geometry, Institute of Physics Publishing, Bristol, United Kingdom, 1993, pp. 104-05.
- 26. J.W. Cahn: Acta Metall., 1961, vol. 9, pp. 795-801.
- G.A. Knorovsky, M.J. Cieslak, T.J. Headley, A.D. Romig, and W.F. Hammetter: Metall. Trans. A, 1989, vol. 20A, pp. 2147-58.
- H.L. Eiselstein: Advances in the Technology of Stainless Steels, ASTM STP 369, ASTM, Philadelphia, PA, 1965, pp. 62-79.

The authors

Viola L. Acoff Department of Metallurgical and Materials Engineering, University of Alabama, Box 870202, Tuscaloosa, Alabama 35487 (vacoff@coe.eng.ua.edu). Dr. Acoff received her B.S. (1989), M.S. (1991), and Ph.D. (1994) degrees in materials engineering from the University of Alabama at Birmingham. She then joined the University of Alabama in Tuscaloosa as Assistant Professor of Metallurgical and Materials Engineering. Professor Acoff teaches undergraduate and graduate courses in welding metallurgy, physical metallurgy, and scanning electron microscopy, and has an active research group that consists of three graduate and four undergraduate students. Her research interests include microstructural evolution of the fusion- and heat-affected zones in materials, high-temperature materials, and electron microscopy; her current research activities involve the weldability and computer modeling of gamma titanium aluminide, the effect of orientation on weld properties, the indentation behavior of materials, particularly joining and interfacial structures, and the processing of alloys by cold roll welding. Dr. Acoff has received numerous awards and recognitions, including the following: the Adams Memorial Membership Award for outstanding teaching activities (2000), the Best Paper Award for the TMS Symposium on Gamma Titanium Aluminides (1999), recognition as the TMS Young Leader Intern (1998), the National Science Foundation CAREER Award (1997), the Warren F. Savage Memorial Award for Best Paper (1996), the IBM Corporation Award for Excellence (1992), and the First Place Award for Best Physical Sciences Paper (1991) from the Microscopy Society of America. She is a member of the American Welding Society, the Minerals, Metals and Materials Society (TMS), the American Society for Materials International, Tau Beta Pi, and Sigma Xi.

Raymond G. Thompson Department of Materials and Mechanical Engineering, University of Alabama at Birmingham, Birmingham, Alabama 35294 (rthompson@eng.uab.edu). Dr. Thompson received his B.S. and M.S. degrees in materials engineering at the University of Alabama at Birmingham (UAB). He received his Ph.D. degree in 1978 from the Department of Materials Science and Engineering at Vanderbilt University. From 1978 to 1981, Professor Thompson taught at Clemson University in the Materials Engineering program of the Department of Ceramic Engineering. Since then he has served on the faculty of the Department of Materials and Mechanical Engineering at UAB. He has served both as the UAB Director of the joint UAB-University of Alabama Materials Science and Engineering Graduate Program and as the UAB Director of the Alabama System Materials Science Graduate Program. Professor Thompson teaches courses in materials selection and design, mechanical deformation of materials, welding metallurgy, surfaces and interfaces, and solid-state diffusional transformation. His research interests are in the field of physical metallurgy involving processing and the modeling and verification of microstructure-property relationships resulting from processing operations. He serves on many committees and has chaired the Metals and Ceramics Committee of the Joining Division Council of the American Society for Materials and the High Temperature Alloys Committee of the Welding Research Council.

Publication of this paper

This paper was originally published on pages 2692-2703 of *Metallurgical and Materials Transactions*, Volume 27A, Number 9 (1996) [Copyright © 1996 by the Minerals, Metals and Materials Society and ASM International.]. It was produced by scanning the original version and contains added biographical sketches of its authors. We gratefully acknowledge permission to include it in this issue.